Zeitschrift: Schweizerische mineralogische und petrographische Mitteilungen = Bulletin suisse de minéralogie et pétrographie

Band: 78 (1998)

Heft: 3

Artikel: Ordovician Barrow-type metamorphism in the Strona-Ceneri Zone (Nothern Italy) dated by U-Pb on staurolite

Autor: Romer, Rolf R. / Franz, Leander

DOI: https://doi.org/10.5169/seals-59296

SCHWEIZ. MINERAL. PETROGR. MITT. 78, 383–395, 1998

Ordovician Barrow-type metamorphism in the Strona-Ceneri Zone (Northern Italy) dated by U–Pb on staurolite

by *Rolf L. Romer*[1] and *Leander Franz*[1,2]

Abstract

The crustal segment of the Strona-Ceneri Zone (SCZ) in northern Italy shows a complex polymetamorphic evolution that is bracketed by the emplacement age of 450–460 Ma old granitoids and the Middle Carboniferous age of mica and amphibole presumably related with the D3-phase. The age of the strongest tectonometamorphic event (D2) in the SCZ, which took place under amphibolite facies conditions at 600 ± 30 °C and 8 ± 1 kbar, resulted in the growth of abundant syntectonic staurolite in a garnet mica schist formed during the D2 clockwise prograde P-T evolution that is typical for Barrow-type metamorphism. The U–Pb and Pb–Pb systematics of staurolite demonstrate that staurolite formed during an Ordovician event and had lost lead during a Variscan overprint. Lead loss occurred preferably from microfractures and crystal defects, whereas lead from structural sites seems not to have been affected. The staurolite gives an Ordovician age for the D2 event, which implies that the metamorphic and structural memory of the SCZ was acquired during at least two distinct tectonometamorphic events.

Keywords: Strona-Ceneri Zone, Southern Alps, U–Pb, staurolite, Ordovician, tectonometamorphism.

Introduction

Radiometric age determination in polymetamorphic terranes is often problematic. (1) Minerals with high closing temperatures such as monazite and zircon commonly cannot be related uniquely to a mineral assemblage distinctive for certain P-T conditions. Therefore, the age obtained from such accessory minerals cannot always be related uniquely with one of the tectonometamorphic events reflected in the mineral assemblage. (2) Minerals such as amphibole and mica, which are easily related to critical mineral assemblages, have closing temperatures for the Rb–Sr, K–Ar, and ^{39}Ar–^{40}Ar systems, depending on the obtained metamorphic grade of the rock, that may be lower than the crystallization temperature of the mineral. The ages obtained from these minerals may represent minimum ages for this event rather than true ages.

These limitations of geochronometers leave space for conflicting interpretations: The crustal segment of the Strona-Ceneri Zone (SCZ) in northern Italy shows a complex polymetamorphic evolution bracketed by the emplacement age of 450–460 Ma old granitoids and Middle Carboniferous ages for mica and amphibole presumably related with the D3-phase (ZURBRIGGEN et al., 1997). The age of the strongest tectonometamorphic event in the SCZ (D2 in ZURBRIGGEN et al., 1997; D1 in BORIANI and VILLA, 1997), which took place under amphibolite facies conditions of 600 ± 30 °C and 8 ± 1 kbar, is debated. ZURBRIGGEN et al. (1997) interpret the Barrow-type metamorphism associated with the D2 event as an Ordovician event. The cooling ages on mica and amphibole as well as Pb–Pb ages on garnet of D3 deformed dikes (ZURBRIGGEN et al., 1998) demonstrate a second tectonometamorphism in mid-Carboniferous. This implies that the structural and metamorphic scenario in the Strona-Ceneri Zone was acquired during at least two unrelated orogenic events. In contrast, BORIANI and VILLA (1997) related the entire structural and metamorphic memory of rocks in the SCZ to one single Variscan tectonothermal event. The problem in part arises from the contrasting interpretation of radiometric ages. ZURBRIGGEN et al. (1997) inter-

[1] GeoForschungsZentrum Potsdam, Telegrafenberg, D-14473 Potsdam, Germany. <romer@gfz-potsdam.de>
[2] Institute of Mineralogy, TU Bergakademie Freiberg, Brennhausgasse 14, D-09596 Freiberg, Germany.

pret the monazite U–Pb ages as the time of metamorphism and the K–Ar and ^{39}Ar–^{40}Ar ages as minimum ages after a second metamorphism. In contrast, BORIANI and VILLA (1997) interpret the K–Ar and ^{39}Ar–^{40}Ar ages as crystallization ages and refer to the older U–Pb ages as irrelevant to the metamorphism.

Controversies of this kind can be resolved or could be avoided if the dated minerals (1) are uniquely related to the structures of interest and (2) are dated by a method that remains a closed system to temperatures significantly higher than the thermal peak experienced by the dated rock. For the SCZ, staurolite represents such a mineral. Staurolite forms (1) a major constituent of S2 structures (as used by ZURBRIGGEN et al., 1997), (2) has a blocking temperature for the U–Pb system that is higher than the thermal maximum experienced by its host rock (see DAHL, 1997), and (3) has no inherited components. We demonstrate that staurolite yields an Ordovician age, which supports claims that the metamorphic and structural memory of the SCZ was acquired during at least two unrelated orogenic events and refutes models that rule out a pre-Variscan structural and metamorphic history of the SCZ.

Relation between Ivrea-Verbano Zone (IVZ) and Strona-Ceneri Zone (SCZ)

The Ivrea Crustal Section is located in northern Italy and forms a part of the pre-Alpine basement of the Southern Alps (Fig. 1). The section, which has a length of about 150 km and a width of up to 60 km, is bound to the northwest by the Insubric Line. In the south, the basement rocks of the Ivrea Crustal Segment are overlain by Permo-Carboniferous sedimentary and volcanic rocks and Mesozoic shelf sequences. The segment is subdivided in the Ivrea-Verbano Zone (IVZ) to the northwest and the Strona-Ceneri Zone (SCZ) to the southeast. IVZ and SCZ are separated by the Pogallo Line, which has been interpreted as a major tilted normal fault zone (HODGES and FOUNTAIN, 1984; HANDY, 1987) and the Cossato-Mergozzo-Brissago (CMB) Line (BORIANI et al., 1990). The protoliths of the IVZ metamorphic

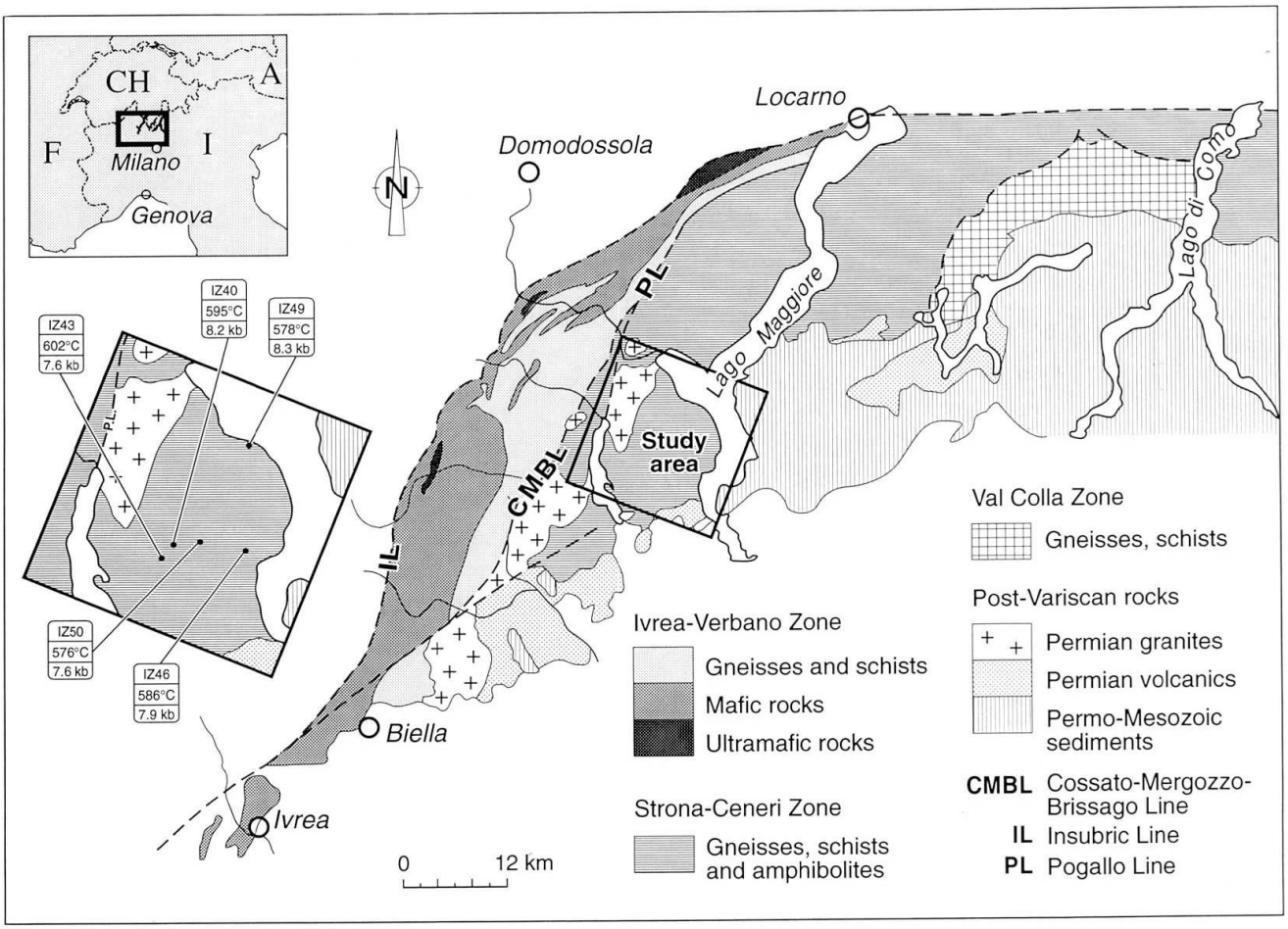

Fig. 1 Geographic position of the Ivrea crustal segment with sample location (centered) and peak metamorphic conditions of the selected mica schists.

rocks were probably deposited/erupted in an accretionary wedge (HANDY et al., in press). The only age estimate for the volcanism and sedimentation in the IVZ originates from SHRIMP analyses on 350 Ma old cores in zircon (VAVRA et al., 1996, see also U–Pb zircon data of KÖPPEL and GRÜNENFELDER [1971, 1978]). The IVZ experienced intense Permo-Carboniferous underplating by mafic and intermediate intrusive rocks at the mantle-crust boundary (HANDY and ZINGG, 1991). Strong thermal effects related with the magmatic underplating and the penetrative extensional deformation in the overlying metamorphic rocks led to the re-equilibration of most geothermobarometers and geochronometers (HENK et al., 1997). Relics of the pre-underplating evolution of the IVZ are limited to the southeastern border of the zone and include kyanite overgrown by sillimanite in paragneiss (BERTOLANI, 1959; CAPEDRI, 1971; BORIANI and SACCHI, 1973; HANDY, 1986) and rare, strongly altered coronas around garnet (BORIANI and PEYRONEL PAGLIANI, 1968). These relics indicate an early, pre- to syn-accretionary phase of subduction and pressure-dominated metamorphism in the IVZ (see HANDY et al., in press).

Similar to the IVZ, the SCZ was affected by a multistage tectonometamorphic evolution. The earliest records of metamorphism in the SCZ, however, are distinctly older than in the IVZ. The protoliths of the Strona-Ceneri sediments probably were part of a Late-Proterozoic to Early Paleozoic subduction accretion complex that was intruded by Ordovician granitoids (ZURBRIGGEN et al., 1997). Xenoliths within these granitoids include relics of MOR-basalts that experienced eclogite-facies metamorphism and paragneisses that underwent D1 deformation under amphibolite-facies conditions. These eclogite and D1-metasediment xenoliths show a penetrative D2 deformation under prograde amphibolite-facies conditions. Textural criteria in the orthogneisses and the adjacent metasediments demonstrate that these granitoids intruded during D2 (ZURBRIGGEN et al., 1997). Therefore, the age of deformation D2 is given by the U–Pb age of zircon and monazite of e.g. the Giumello gneiss dated at 457 ± 4 Ma (discordia intercept, RAGETTLI, 1993) and 450 ± 10 Ma (KÖPPEL and GRÜNENFELDER, 1971) and the Ceneri gneiss dated at 456 ± 4 Ma (concordant, RAGETTLI, 1993). P-T conditions during this event are estimated at 570–630 °C and 7–9 kbar (FRANZ et al., 1996; ZURBRIGGEN et al., 1997). The SCZ was overprinted by large scale D3 folds at ca 330 Ma (ZURBRIGGEN et al., 1998), so called "Schlingen", that formed under lower amphibolite-facies conditions (500–550 °C, 4–5 kbar; see FRANZ et al., 1996; HANDY et al., in press). The D3-event, which may be related to the tectonic underplating/accretion of the IVZ with the SCZ, was accompanied by dike-magmatism and wiped out the geochronological features of the preceding D2 event in wide parts of the SCZ (HANDY et al., in press). The border zone of the SCZ was additionally affected by the thermal effects of the Permo-Carboniferous and Triassic magmatic underplating in the IVZ (ZINGG, 1983; VON QUADT et al., 1993; FRANZ et al., 1994; HENK et al., 1997; HANDY et al., in press). Similar to the IVZ, the SCZ only experienced an Alpine sub-greenschist facies overprint (ZINGG, 1990).

Despite these abundant textural, petrologic, and geochronological constraints that indicate a pre-Variscian age for D1 and D2, the metamorphic evolution of the SCZ is a matter of controversy. D3 in the SCZ is related to the amalgamation of the Ivrea-Verbano segment with the Strona-Ceneri segment (HANDY et al., in press). D2 and D1, however, are by some groups interpreted as early phases of docking of IVZ and SCZ and thus of Permo-Carboniferous age (e.g., SCHMID, 1993; BORIANI and VILLA, 1997), whereas ZURBRIGGEN et al. (1997) and other groups argue that these structures originate from a distinctly older orogenic event.

Petrologic characterization of the D2 event

Strong reworking of large parts of the SCZ during the D3 tectonometamorphic event, local reheating during the Upper Carboniferous magmatic underplating from the IVZ, and local contact metamorphism near the Permian Baveno-type granites, give the SCZ a complex polydeformative and polymetamorphic character that makes it difficult to find samples suited to date unequivocally pre-D3 metamorphism. However, in the area between Lago d'Orta and Lago Maggiore east of the city of Omegna (Fig. 1), these effects are absent or only weakly developed. There occur monotonous successions of metapelites (mainly garnet-staurolite mica schists) and interlayering garnet-bearing gneisses of psammitic origin. Metasediments in this region mainly carry the textural features of the D2-deformation, i.e., isoclinal folds, with a penetrative S2 schistosity, a uniformly N–S directed stretching lineation, and rotated garnets and syntectonic staurolite, mica, as well as plagioclase.

Five garnet mica schists along a profile from Armeno in the NW to Stresa near the Lago Maggiore (see Fig. 1) were selected and investigated with the microprobe. Two samples are garnet-chlorite mica schists (GC-Ms) which show an alignment of the mineral assemblage Grt + Bt +

Tab. 1 Microprobe analyses of garnet, biotite and staurolite.

Garnet	IZ43	IZ43	IZ40	IZ50	IZ50	IZ50	IZ49	IZ46
	GS-Ms	GS-Ms	GS-Ms	GS-Ms	GS-Ms	GS-Ms	GC-Ms	GC-Ms
wt.-%	near rim	core mG	near rim	core	near rim	rim	near rim	near rim
SiO_2	37.32	37.44	37.36	36.84	37.34	37.22	37.59	36.52
TiO_2	0.09	0.05	0.04	0.10	0.00	0.01	0.05	0.12
Al_2O_3	21.42	21.31	21.25	21.43	21.50	21.19	20.62	21.13
Cr_2O_3	0.03	0.04	0.00	0.03	0.03	0.02	0.04	0.02
Fe_2O_3	0.45	0.00	0.48	0.42	0.17	0.00	0.67	1.00
MgO	3.40	3.23	3.26	2.26	3.33	3.09	2.72	3.25
CaO	2.12	2.24	2.31	5.12	2.82	0.92	3.48	2.79
MnO	1.38	1.71	2.70	2.71	1.11	1.67	2.35	2.36
FeO	35.09	33.96	33.60	31.61	34.46	36.11	32.92	33.05
Na_2O	0.01	0.03	0.00	0.01	0.00	0.02	0.03	0.01
Total:	101.30	100.01	100.99	100.52	100.77	100.23	100.46	100.26
Cations (O=12)								
Si	2.965	3.000	2.977	2.951	2.974	2.995	3.011	2.937
Ti	0.005	0.003	0.002	0.006	0.000	0.001	0.003	0.007
Al	2.006	2.013	1.996	2.023	2.018	2.009	1.946	2.003
Cr	0.002	0.002	0.000	0.002	0.002	0.001	0.002	0.001
Fe^{3+}	0.027	0.000	0.029	0.025	0.010	0.000	0.041	0.061
Mg	0.403	0.386	0.387	0.270	0.395	0.370	0.325	0.390
Ca	0.181	0.193	0.197	0.439	0.241	0.079	0.299	0.240
Mn	0.093	0.116	0.182	0.184	0.075	0.114	0.159	0.161
Fe^{2+}	2.331	2.276	2.239	2.117	2.295	2.430	2.205	2.223
Na	0.001	0.005	0.000	0.002	0.000	0.004	0.004	0.002
Total:	8.013	7.990	8.009	8.019	8.011	8.019	7.996	8.025
Endmembers:								
Uvar:	0.09	0.12	0.00	0.09	0.10	0.05	0.12	0.07
Adr:	0.26	0.15	0.39	0.29	0.11	0.04	2.18	0.39
Grs:	5.67	6.21	6.17	14.22	7.80	2.55	7.70	7.51
Alm:	77.52	76.61	74.50	70.33	76.34	81.19	73.80	73.76
Sps:	3.08	3.91	6.06	6.11	2.50	3.80	5.33	5.33
Prp:	13.39	12.99	12.88	8.98	13.15	12.37	10.86	12.95

Biotite	IZ43	IZ43	IZ40	IZ50	IZ49	IZ46
	GS-Ms	GS-Ms	GS-Ms	GS-Ms	GC-Ms	GC-Ms
wt.-%	core	core spp	core	core	core	core
SiO_2	36.53	36.22	35.42	36.36	36.64	35.40
TiO_2	1.81	1.67	1.71	1.45	1.61	1.50
Al_2O_3	18.60	19.01	19.69	18.10	18.95	18.77
Cr_2O_3	0.00	0.04	0.00	0.00	0.00	0.00
MgO	10.68	10.60	10.52	11.43	10.15	11.36
CaO	0.00	0.00	0.00	0.00	0.00	0.00
MnO	0.09	0.00	0.07	0.15	0.08	0.06
FeO	19.04	18.90	18.12	18.45	18.68	18.50
BaO	0.00	0.00	0.10	0.05	0.00	0.06
Na_2O	0.15	0.26	0.22	0.13	0.11	0.11
K_2O	8.84	8.65	8.87	9.22	8.84	9.10
H_2O	3.78	3.789	3.68	3.72	3.77	3.68
F	0.39	0.38	0.54	0.48	0.40	0.54
Cl	0.08	0.04	0.08	0.06	0.05	0.03
Total:	99.99	99.56	99.01	99.60	99.28	99.10
Total c.:	99.81	99.39	98.77	99.38	99.10	98.87
Cations (O=12)						
Si	2.745	2.729	2.687	2.749	2.765	2.692
Ti	0.103	0.095	0.098	0.082	0.091	0.086
Al	1.647	1.688	1.760	1.613	1.686	1.683
Cr	0.000	0.002	0.000	0.000	0.000	0.000
Mg	1.196	1.191	1.189	1.288	1.142	1.288
Ca	0.000	0.000	0.000	0.000	0.000	0.000
Mn	0.006	0.000	0.004	0.010	0.005	0.004
Fe	1.197	1.191	1.149	1.167	1.179	1.177
Ba	0.000	0.000	0.003	0.002	0.000	0.002
Na	0.021	0.038	0.032	0.019	0.016	0.016
K	0.847	0.831	0.858	0.889	0.851	0.883
Total:	7.763	7.766	7.780	7.817	7.735	7.830
OH	1.897	1.904	1.860	1.877	1.898	1.867
F	0.093	0.091	0.130	0.115	0.095	0.129
Cl	0.010	0.005	0.010	0.008	0.006	0.004

Stauro-lite	IZ43	IZ40	IZ50	IZ50
	GS-Ms	GS-Ms	GS-Ms	GS-Ms
wt.-%	rim	rim	core	rim
SiO_2	28.71	27.71	28.97	28.67
TiO_2	0.66	0.63	0.61	0.75
Al_2O_3	54.53	54.47	53.56	53.67
Cr_2O_3	0.07	0.09	0.00	0.03
MgO	1.52	1.41	1.95	1.57
CaO	0.00	0.00	0.01	0.00
MnO	0.25	0.38	0.18	0.43
FeO	12.29	11.99	13.14	12.79
CuO	0.00	0.00	0.00	0.00
ZnO	0.50	1.94	0.42	0.50
BaO	0.00	0.00	0.00	0.00
Na_2O	0.01	0.06	0.03	0.00
K_2O	0.00	0.02	0.01	0.01
Total:	98.53	98.68	98.89	98.00
Cations (O=23)				
Si	3.930	3.824	3.967	3.945
Ti	0.068	0.065	0.063	0.077
Al	8.797	8.857	8.644	8.703
Cr	0.007	0.009	0.000	0.003
Mg	0.310	0.290	0.399	0.321
Ca	0.000	0.000	0.002	0.000
Mn	0.029	0.044	0.020	0.050
Fe	1.407	1.383	1.505	1.472
Cu	0.000	0.000	0.000	0.000
Zn	0.050	0.197	0.043	0.051
Ba	0.000	0.000	0.000	0.000
Na	0.002	0.015	0.008	0.000
K	0.000	0.003	0.001	0.002
Total:	14.601	14.687	14.653	14.625

Tab. 2 Microprobe analyses of plagioclase, muscovite and chlorite.

Plagio-clase	IZ43 GS-Ms	IZ43 GS-Ms	IZ40 GS-Ms	IZ50 GS-Ms	IZ50 GS-Ms	IZ50 GS-Ms	IZ49 GC-Ms	IZ46 GC-Ms
wt.-%	rim	core stp.	rim	core inc	nr inc.	rim	rim	rim
SiO_2	65.41	64.12	64.44	63.57	64.99	65.27	64.82	63.02
Al_2O_3	21.80	22.23	21.09	22.41	22.20	21.67	21.78	22.41
MgO	0.00	0.00	0.01	0.00	0.00	0.00	0.00	0.02
CaO	3.68	3.58	3.17	4.39	4.13	3.52	3.93	3.79
MnO	0.00	0.01	0.01	0.03	0.03	0.00	0.02	0.01
FeO	0.03	0.00	0.00	0.52	0.06	0.03	0.05	0.00
BaO	0.00	0.02	0.88	0.00	0.08	0.01	0.12	0.84
Na_2O	9.70	9.47	9.93	9.09	9.57	9.78	9.17	9.18
K_2O	0.09	0.06	0.03	0.38	0.10	0.27	0.10	0.09
Total:	100.71	99.49	99.56	100.37	101.17	100.55	99.99	99.37
Cations (O=8)								
Si	2.863	2.840	2.871	2.810	2.840	2.864	2.859	2.816
Al	1.124	1.161	1.107	1.168	1.143	1.121	1.132	1.180
Mg	0.000	0.000	0.001	0.000	0.000	0.000	0.000	0.001
Ca	0.172	0.170	0.151	0.208	0.193	0.165	0.185	0.181
Mn	0.000	0.000	0.000	0.001	0.001	0.000	0.001	0.001
Fe	0.001	0.000	0.000	0.019	0.002	0.001	0.002	0.000
Ba	0.000	0.000	0.015	0.000	0.001	0.000	0.002	0.015
Na	0.823	0.813	0.858	0.779	0.811	0.832	0.784	0.795
K	0.005	0.003	0.002	0.021	0.006	0.015	0.006	0.005
Total:	4.989	4.988	5.005	5.006	4.997	4.999	4.970	4.994
Endmembers:								
An:	17.24	17.22	14.75	20.61	19.11	16.33	18.98	18.20
Ab:	82.24	82.41	83.59	77.28	80.19	82.15	80.22	79.78
Or:	0.52	0.34	0.17	2.10	0.56	1.50	0.58	0.54
Ce:	0.00	0.04	1.50	0.00	0.14	0.02	0.22	1.48

Musco-vite	IZ43 GS-Ms	IZ43 GS-Ms	IZ40 GS-Ms	IZ50 GS-Ms	IZ49 GC-Ms	IZ46 GC-Ms
wt.-%	core	core	core	core	core	core
SiO_2	47.01	47.16	45.40	47.17	47.13	46.87
TiO_2	0.61	0.55	0.52	0.51	0.35	0.49
Al_2O_3	35.79	35.70	36.65	36.36	35.77	37.09
Cr_2O_3	0.00	0.02	0.00	0.01	0.03	0.00
MgO	0.58	0.64	0.62	0.60	0.61	0.66
CaO	0.00	0.00	0.00	0.01	0.00	0.00
MnO	0.02	0.02	0.00	0.01	0.00	0.00
FeO	0.79	0.84	0.77	0.87	0.87	0.85
BaO	0.19	0.20	0.26	0.00	0.47	0.24
Na_2O	2.10	1.51	2.21	2.78	1.35	2.08
K_2O	8.10	9.59	7.93	7.42	8.36	8.19
Total:	95.19	96.23	94.36	95.74	94.95	96.48
Cations (O=11)						
Si	3.096	3.095	3.022	3.080	3.113	3.049
Ti	0.030	0.027	0.026	0.025	0.017	0.024
Al	2.778	2.761	2.876	2.798	2.785	2.844
Cr	0.000	0.001	0.000	0.000	0.001	0.000
Mg	0.057	0.063	0.062	0.059	0.060	0.064
Ca	0.000	0.000	0.000	0.001	0.000	0.000
Mn	0.001	0.001	0.000	0.001	0.000	0.000
Fe	0.043	0.046	0.043	0.048	0.048	0.046
Ba	0.005	0.005	0.007	0.000	0.012	0.006
Na	0.268	0.192	0.285	0.352	0.173	0.263
K	0.681	0.803	0.674	0.618	0.704	0.680
Total:	6.959	6.994	6.994	6.980	6.915	6.976
Endmembers:						
Mrg:	0.00	0.00	0.00	0.07	0.02	0.00
Pg:	28.26	19.31	29.75	36.24	19.72	27.89
Cel:	9.60	9.49	2.19	7.97	11.34	4.91
Ms:	62.15	71.20	68.06	55.72	68.92	67.20

Chlorite	IZ43 GS-Ms	IZ40 GS-Ms	IZ50 GS-Ms	IZ49 GC-Ms	IZ46 GC-Ms
wt.-%	core	core	core	core	core
SiO_2	24.96	25.18	26.12	25.54	25.54
TiO_2	0.05	0.07	0.06	0.10	0.10
Al_2O_3	23.92	23.83	23.81	22.17	22.81
MgO	13.39	15.97	14.28	15.27	15.76
CaO	0.01	0.00	0.01	0.01	0.00
MnO	0.16	0.10	0.28	0.19	0.16
FeO	26.14	23.49	25.43	24.27	23.35
Na_2O	0.03	0.02	0.05	0.01	0.04
K_2O	0.04	0.01	0.08	0.05	0.10
Total:	88.69	88.68	90.12	87.61	87.86
Cations (O=28)					
Si	5.204	5.178	5.326	5.349	5.305
Ti	0.008	0.011	0.009	0.016	0.016
Al	5.877	5.775	5.722	5.473	5.583
Mg	4.161	4.896	4.341	4.768	4.879
Ca	0.003	0.000	0.002	0.002	0.000
Mn	0.027	0.018	0.048	0.033	0.028
Fe	4.558	4.038	4.336	4.251	4.055
Fe	0.000	0.000	0.000	0.000	0.000
Na	0.011	0.007	0.020	0.005	0.016
K	0.010	0.003	0.021	0.012	0.028
Total:	19.860	19.928	19.824	19.908	19.910

Ms + Chl + Pl ± Rt, Ilm within the S2 schistosity. Three samples are garnet-staurolite mica schists (GS-Ms) with the syntectonic D2 mineral assemblage Grt + St + Bt + Ms + Chl + Pl ± Rt, Ilm.

Garnet from the GC-Ms displays compositional growth zoning with bell shaped patterns for Mn and Ca and progressively increasing Fe- and Mg-contents from core to rim. In near rim sections, garnet yields the highest X_{Mg} – (= Mg/(Mg + Fe) values (0.86–0.88) and shows a composition of $Alm_{73-14}Prp_{11-13}Grs_{7-8}Sps_{5-6}$. Plagioclase is also often zoned with core compositions of An_{04-06} steadily increasing to An_{18-19} at the rim, whereas sheet silicates are unzoned (see Tab. 1 and 2 for mineral compositions).

Two generations of garnet are present in most GS-Ms: large garnets (> 1 cm) have bell-shaped Mn- and Ca-zonation patterns similar to the garnet from GC-Ms and display the highest X_{Mg}-values (0.85–0.86) near the rim (see Tab. 1). At the outermost part of the rim, a decrease of the pyrope content at the expense of almandine and spessartine components points to retrograde cooling. The second generation of garnet occurs as small, idioblastic inclusions with diameters of 0.1–0.2 mm in large, aligned plagioclase grains. These small garnets yield similar X_{Mg}-values and compositions as the rims of the large garnet grains. They are believed to have grown syntectonically near the peak of D2 metamorphism. Prismatic staurolite is always distinctly aligned in the S2 foliation (Fig. 2) and shows increasing X_{Fe} – (= Fe/(Fe + Mg) values from core to rim (see Tab. 1). Plagioclase in the GS-Ms is either unzoned or shows a slight decrease in An from core to rim (i.e., An_{22}–An_{16}). This zonation is present in plagioclase inclusions in the bigger garnets. Mineral compositions of plagioclase as well as the sheet silicates of the GS-Ms are listed in tables 1 and 2.

Peak metamorphic temperatures for the D2 event in GC-Ms and GS-Ms, estimated with the Grt-Bt-geothermometer of HODGES and SPEAR (1982), the Grt-St-geothermometer of PERCHUK (1969) and the Grt-Chl-geothermometer of GHENT et al. (1987), were in the range of 570–610 °C. Metamorphic pressures were at 7.4–8.4 kbar (Fig. 1) according to the Grt-Ms-Bt-Plg-geobarometer of HOISCH (1989; calibration P1) and is in accordance with the calibration of POWELL and HOLLAND (1988) and the GRIPS geobarometer of BOHLEN and LIOTTA (1986). Sample IZ50 allows a determination of a clockwise, prograde P-T-t path (see Fig. 3) using plagioclase inclusions in the garnet core (An_{21}), in the near rim section of the garnet (An_{19}) and a plagioclase rim (An_{16}) adjacent to the retrograde rim section of garnet in

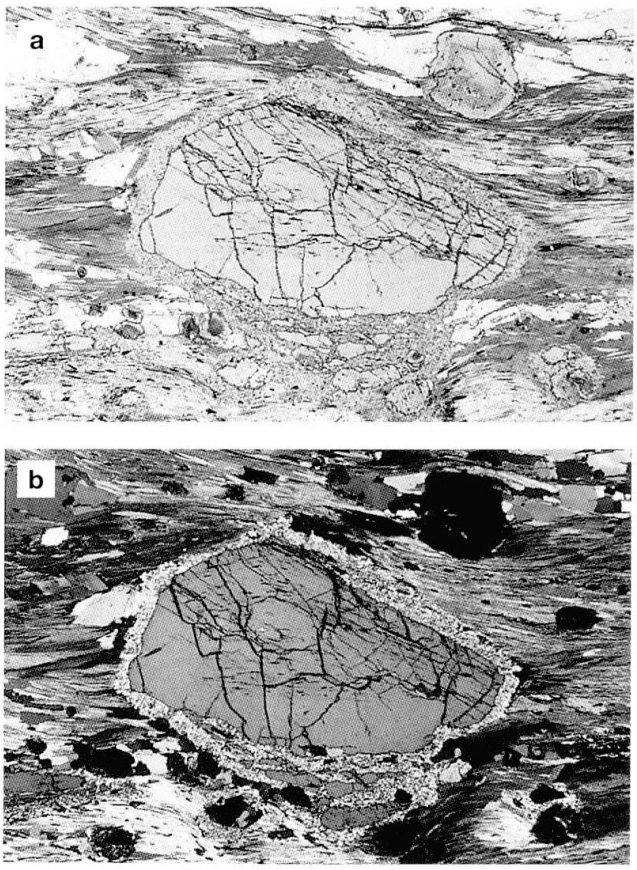

Fig. 2 Microphotograph of syntectonic staurolite with inclusion trails of ilmenite, rutile, and graphite aligned in the D2 foliation along with garnet, biotite, muscovite, plagioclase, and quartz. Photograph with crossed nicols distinctly shows decomposition of the staurolite to chlorite and mica at its rim. Length of lower edge is 7 mm.

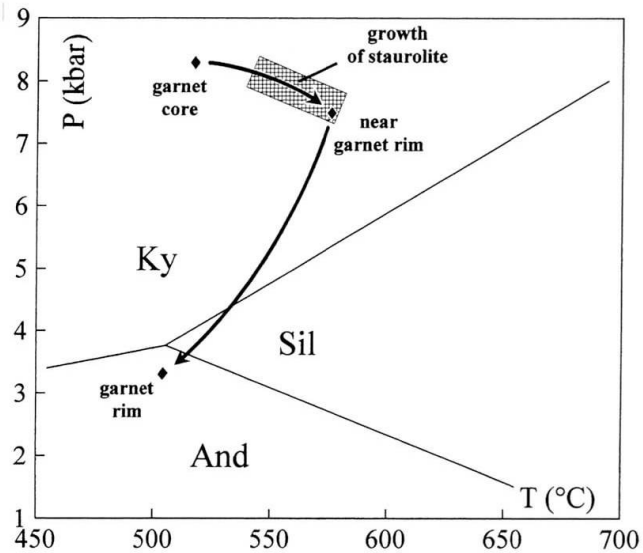

Fig. 3 P-T path for the D2 event derived by garnet-biotite thermometry of HODGES and SPEAR (1982) and garnet-biotite-muscovite-plagioclase geobarometry of HOISCH (1989).

Tab. 3 U–Pb analytical data of staurolite from a garnet-staurolite mica schist from the Strona-Ceneri Zone, east of Omegna, northern Italy.

Sample[a]	Weight (mg)	Concentrations (ppm)		$^{206}Pb/^{204}Pb$	Radiogenic Pb (at%)[c]			Atomic ratios[c]			Apparent ages (Ma)[d]		
				Measured ratios[b]	^{206}Pb	^{207}Pb	^{208}Pb	$^{206}Pb/^{238}U$	$^{207}Pb/^{235}U$	$^{207}Pb/^{206}Pb$	$^{206}Pb/^{238}U$	$^{207}Pb/^{235}U$	$^{207}Pb/^{206}Pb$
		U	Pb_{tot}										
Common lead $^{206}Pb/^{204}Pb = 18.77 \pm .07$, $^{207}Pb/^{204}Pb = 15.67 \pm .02$, $^{208}Pb/^{204}Pb = 37.77 \pm .07$													
St1	6.455	0.603	0.234	34.066	36.60	2.01	61.39	.06150	.46576	.05493	385	388	409
St2	3.258	3.789	1.015	44.514	37.96	2.17	59.87	.05735	.45257	.05724	360	379	501

[a] Staurolite concentrates were obtained by separating millimeter large grains from the garnet-staurolite-mica schist, crushing these grains and separating the fragments by hand under the binocular. Care was taken to use only fragments with fracture surfaces to avoid the thin films of plagioclase and retrograde chlorite that have formed locally on grain surfaces. All analyzed fragments were optically clear and inclusion-free. Both samples were dissolved with 52% HF in Savillex beakers at 220 °C for six days on the hot plate, dried, and transferred into chloride-form using 6N HCl. Ion-exchange chromatography, after aliquotting by weight and tracer-addition, as described by TILTON (1973) and MANHÈS et al. (1978). Measured on single Re-filaments using a silica-gel emitter and H_3PO_4 (GERSTENBERGER and HAASE, 1997) at 1200–1260 °C on a Finnigan MAT262 multicollector mass-spectrometer using Faraday collectors.

[b] Lead isotope ratios corrected for fractionation with 0.1% / a.m.u.

[c] Lead corrected for fractionation, blank, and initial lead. During the measurement period total blanks were less than 30 pg for lead and less than 1 pg for uranium for samples analyzed with a ^{208}Pb–^{235}U mixed tracer.

[d] Apparent ages were calculated using the constants of JAFFEY et al. (1971) recommended by IUGS (STEIGER and JÄGER, 1977).

combination with muscovite and biotite from the matrix. These results agree with the contoured petrogenetic grid of SPEAR and CHENEY (1989), with the geothermometry of POWNCEBY et al. (1987 a, b) on ilmenite inclusions in garnet, and the GRIPS-geobarometer of BOHLEN and LIOTTA (1986).

U–Pb and Pb–Pb systematics of staurolite

Two staurolite samples have been analyzed using U–Pb (Tab. 3). The distribution of uranium and common lead in staurolite seems to be heterogeneous as indicated by the contents of 0.6 and 3.8 ppm of uranium (Tab. 3) and ca 0.15 and 0.52 ppm of common lead. Because of the common lead content, the isotopic composition of staurolite is not very radiogenic. $^{206}Pb/^{204}Pb$ ratios of the two samples are 34.066 and 44.514 and the corresponding $^{207}Pb/^{204}Pb$ ratios are only 16.508 and 17.081. Consequently, the contributions of initial lead are significant and the $^{207}Pb_{rad}/^{235}U$ and $^{207}Pb_{rad}/^{206}Pb_{rad}$ ratios have rather large errors 2.7–4.7% and 2.6–4.4% respectively. Due to the large uncertainty in the $^{207}Pb_{rad}/^{235}U$ ratio, the data fall in the concordia diagram (Fig. 4) one the concordia. The contrasting $^{206}Pb_{rad}/^{238}U$ ratios, however, indicate that the two samples have not been closed systems, but seem to have lost some lead. Thus, the well-constrained $^{206}Pb/^{238}U$ ages (385 ± 6 Ma and 360 ± 3 Ma, Tab. 3) represent minimum ages for the crystallization of staurolite. The minimum age for the crystallization of staurolite is given by the higher of the two $^{206}Pb/^{238}U$ ages, i.e., 385 ± 6 Ma (Tab. 3; Fig. 4). The staurolite minimum age supports K–Ar hornblende ages between 346 Ma and 389 Ma from the northeastern part of the SCZ that have been interpreted to yield minimum ages for a pre-Variscan event (MCDOWELL, 1970). Notably, both staurolite minimum ages and

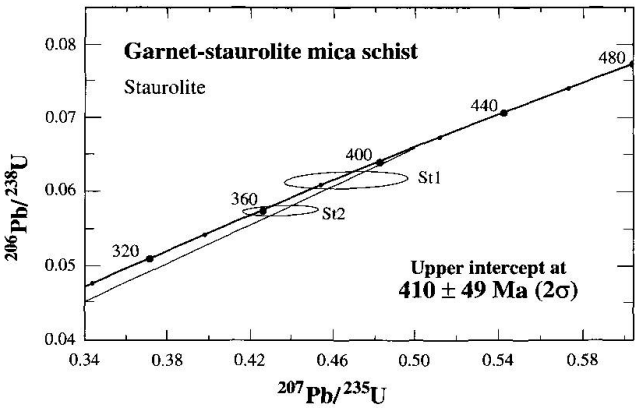

Fig. 4 Concordia diagram for staurolite bulk-samples St1 and St2. The contrasting $^{206}Pb/^{238}U$ age of the two fractions indicates lead loss. The intercept age of 410 ± 49 Ma is calculated from a discordia fitted through the origin of the diagram and represents a minimum age.

the pioneering K–Ar hornblende ages of McDOWELL (1970) are beyond error higher than the $^{39}Ar/^{40}Ar$ ages on amphibole and mica from rocks of the southwestern part of the SCZ (BORIANI and VILLA, 1997).

A third staurolite sample was leached with successively stronger acids and the lead isotopic composition of the leachates was analyzed (Tab. 4). The leaching procedure (Tab. 4) follows the one of FREY and KAMBER (1995). The idea of this leaching procedure is: (1) For grains that were closed systems after crystallization, the lead data should fall on a straight line, whose slope $^{207}Pb/^{206}Pb$ only depends on the age of the mineral. (2) Lead incorporated in the crystal structure, located on fractures and grain surfaces, and formed by radioactive decay of uranium and thorium behave differently during leaching. Lead on surfaces and on structural sites damaged by radioactive decay are more easily leached than lead incorporated into the crystal structure. Lead that is easily leached by weak acids most likely also represents those lead contributions most easily affected by later metamorphic processes and weathering.

The lead isotope data of the various leachates from the staurolite do not fall on a common straight line in the $^{206}Pb/^{204}Pb$–$^{207}Pb/^{204}Pb$ and $^{206}Pb/^{204}Pb$–$^{208}Pb/^{204}Pb$ diagrams, which agrees with the U–Pb data that also indicate some minor post-crystallization disturbance. The two HBr leachates seem to be the most affected solutions (Fig. 5). Leachate HBr-1 represents a low-temperature leach and most likely has mobilized lead from grain surfaces and fractures (cf. also FREY et al., 1995, 1997). It has the least radiogenic lead isotopic composition of the five solutions. It is distinctive by its – in comparison to the HNO_3, HCl and HF leachates – anomalously high $^{208}Pb/^{204}Pb$ ratio (43.314; Tab. 4, Fig. 5). Leachate HBr-2 has the most radiogenic lead isotopic composition of all leachates. It falls in the $^{206}Pb/^{204}Pb$–$^{207}Pb/^{204}Pb$ diagram below the regression line through the other samples and shows in the $^{206}Pb/^{204}Pb$–$^{208}Pb/^{204}Pb$ diagram similarly high $^{208}Pb/^{206}Pb$ signatures as leachate HBr-1. The lead isotope signature of leachate HBr-2 is compatible with a two-stage evolution, whereby the second stage had a higher μ-value ($^{238}U/^{204}Pb$) than the first one, which corresponds to lead loss or uranium gain. The other three leachates fall on linear trends in the $^{206}Pb/^{204}Pb$–$^{207}Pb/^{204}Pb$ and $^{206}Pb/^{204}Pb$–$^{208}Pb/^{204}Pb$ diagrams; which indicates that they behaved chemically coherent, represent structurally bound lead (HF-leachate is the total dissolution of the residue), and originate from structural sites with similar Th/U.

Tab. 4 Staurolite trace lead isotope data from a garnet-staurolite-mica schist east of Omegna, northern Italy.

Sample[a]	$\frac{^{206}Pb}{^{204}Pb}$[b]	$\frac{^{207}Pb}{^{204}Pb}$[b]	$\frac{^{208}Pb}{^{204}Pb}$[b]
St1	34.066	16.508	63.438
St2	44.514	17.081	78.372
St3-HBr-1	20.417	15.675	43.314
St3-HBr-2	82.172	18.881	152.534
St3-HNO_3	23.213	15.862	38.609
St3-HCl	20.687	15.741	38.229
St3-HF	27.077	16.121	39.599

[a] Bulk staurolite samples St1 and St2. Sample St3 was ground and washed with 0.8 N HBr before leaching with cold 8.8 N HBr for 3 h (in ultrasonic). Other leaching steps were performed on the hot plate: with 8.8 N HBr for 24 h, with 14 N HNO_3 for 24 h, with 6 N HCl for 24 h, and with 52% HF for 72 h.

[b] Lead isotope analyses were performed at GeoForschungsZentrum Potsdam, Germany, using a Finnigan MAT262 multicollector mass spectrometer. The lead isotopic composition is corrected for mass discrimination with 0.1%/a.m.u. 2σ reproducibility is better than 0.1%.

The contrasting $^{208}Pb_{rad}/^{206}Pb_{rad}$ (measured lead corrected for contributions of common lead as indicated in Tab. 3) signature of the HBr-leachates and the other three leachates indicates that Th and U in part are located in different sites in the staurolite crystal. The higher $^{208}Pb_{rad}/^{206}Pb_{rad}$ ratios of the HBr-leachates indicate a Th/U of 13.5 and 7.3 (derived for an age of 450 Ma), whereas the Th/U of the other fractions ranges from 0.76 to 0.96. The easier leached lead, i.e., the lead bound to fractures (cf. Fig. 2) and crystal imperfections, has a higher Th/U than the structurally bound lead. Furthermore, the high Th/U of leachate HBr-2 indicates that most of the thorium is not incorporated in the crystal structure of staurolite, but resides in defects and imperfections. The slope of the lead line corresponds to a $^{207}Pb/^{206}Pb$ age at 282 ± 15 Ma, which falls in the same age range as the post-kinematic Permian intrusions of Baveno, Montorfano, and Mottarone (e.g., PINARELLI et al., 1988). This $^{207}Pb/^{206}Pb$ age is a geologically significant age if (1) the initial common lead of the two HBr-leachates was identical and (2) the geologic disturbance affecting the lead systematics of leachate HBr-2 caused a complete removal of radiogenic lead. Else, the $^{207}Pb/^{206}Pb$ age constrained by these two samples represents a minimum age. In contrast, the $^{207}Pb/^{206}Pb$ age of the lead line through the remaining scattered three samples is 605 Ma (MSWD = 10.5) with a very

large error. Using these three samples and the bulk samples St1 and St2 yields 477 ± 120 Ma (2σ; MSWD = 6.5; uncertainties expanded with square root of MSWD, see e.g., KULLERUD, 1991; LUDWIG, 1994), most of the scatter being due to sample St3-HNO_3 (note, that samples St1 and St2 do no strictily conform with the requirements for a fit to a secondary-lead isochron [e.g., ROMER and BRIDGWATER, 1997] as the bulk-samples have suffered from Variscan lead loss and may reduce the slope and appartent age of the lead line). Alternatively to the interpretations that the two sets of lead data define secondary lead isochrons, the lead lines also could originate from two-stage lead-growth with highly correlated μ_1 and μ_2 values (see SCHIØTTE, 1989; ROMER and BRIDGWATER, 1997). For $\mu_1 < \mu_2$, as inferred from the U–Pb data (lead loss or uranium gain), the

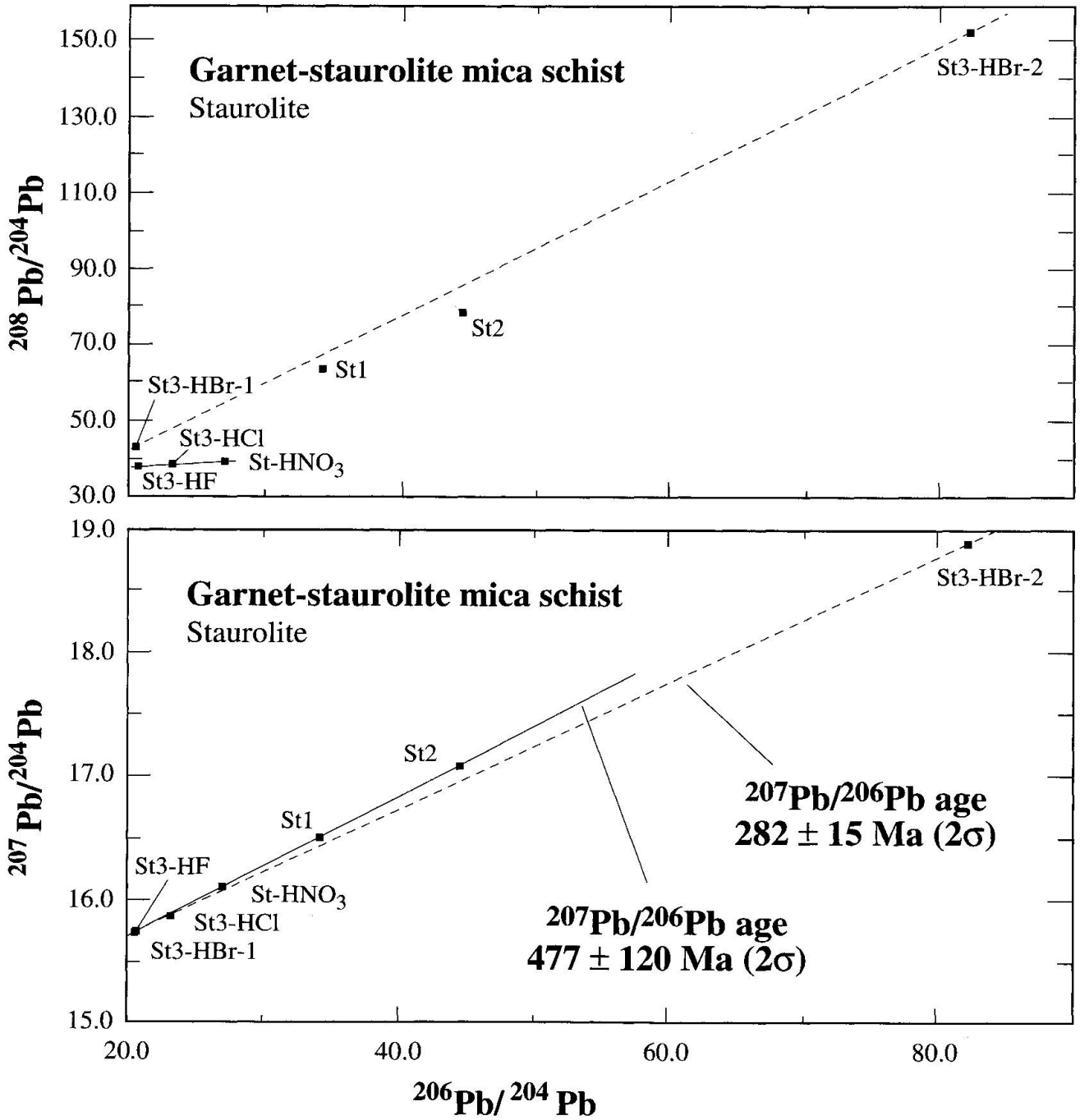

Fig. 5 $^{206}Pb/^{204}Pb$–$^{207}Pb/^{204}Pb$ and $^{206}Pb/^{204}Pb$–$^{208}Pb/^{204}Pb$ diagram for staurolite samples. Note (1) the contrasting $^{207}Pb/^{206}Pb$ slopes of the line St3-HBr-1 to St3-HBr-2 and all other fractions and (2) the contrasting $^{208}Pb/^{206}Pb$ slopes for the HBr leachates and the HNO_3, HCl, and HF leachates and the position of the bulk-samples St1 and St2 between the two lines.

obtained ages at 282 ± 15 and 477 ± 120 Ma would represent minimum ages.

The $^{206}Pb/^{204}Pb$–$^{208}Pb/^{204}Pb$ diagram demonstrates that the lead isotopic signature of the analyzed staurolite is dominated by two components. This is also apparent by the position of the two bulk fractions in that diagram. The samples St1 and St2 represent a weighted mixture of the different leachates and fall correspondingly also between the lead trend of the HBr-leachates and the other leachates (Fig. 5). Furthermore, the presence of two contrasting lead signatures in staurolite also explains the contrasting $^{206}Pb/^{238}U$ ages of the samples St1 and St2 that apparently represent mixed ages between the formation age given by the HNO_3–HCl–HF lead line (ca 477 Ma) and the HBr-1–HBr-2 lead line (ca 282 Ma). The lead systematics of the leached staurolite sample demonstrates unequivocally the presence of two lead components of contrasting age, which implies that the $^{206}Pb/^{238}U$ age at 385 ± 6 Ma of St1 represents a minimum age for the S2-defining metamorphism, and thus, gives proof for a pre-Variscan metamorphism in the SCZ.

Geochronologic, petrologic, and structural arguments for and against a Variscan age of the D2 deformation

The oldest metamorphic rocks in the SCZ are D1-deformed amphibolite-facies metapelites and gneisses, as well as amphibolites with eclogitic relics, which all occur as xenoliths within the Ordovician granitoids. The xenoliths have the same age or are older than the granitoids, which intruded ca. 450–460 Ma ago (KÖPPEL and GRÜNENFELDER, 1971; RAGETTLI, 1993). The D2 foliation at the margin and interior of these intrusive rocks demonstrates that the granitoids were emplaced syntectonic with the formation of this foliation (ZURBRIGGEN et al., 1997). Therefore, the age for D2 structures is given by the emplacement age of the oldest intrusive rocks, i.e., the ca. 450–460 Ma old granitoids (KÖPPEL and GRÜNENFELDER, 1971; RAGETTLI, 1993). The D3 event is dated by Pb–Pb age at 320 Ma on garnet from a synkinematic (D3) dike in the Valle Cannobina (ZURBRIGGEN et al., 1997). Furthermore, the correlation of amphibolite and greenschist-facies structures (D3) in the SCZ with ^{39}Ar–^{40}Ar and Rb–Sr mica and amphibole ages, which close in the range of 300–500 °C indicate that D3 is of Variscan age. Finally, mylonites in the Val Colla Zone overprint D3 structures. The mylonites are dated and constrain the age of D3 to > 320 Ma (cf. HANDY et al., in press).

These data should be argument enough to assign deformation phase D2 (D1 in BORIANI and VILLA, 1997) to a pre-Variscan orogenic event that is entirely unrelated with the docking of the SCZ with the IVZ. However, because of the geographically widespread mica and amphibole ages (K–Ar, ^{39}Ar–^{40}Ar, Rb–Sr) from all kinds of structures in the SCZ (e.g., ZINGG et al., 1990; BORIANI and VILLA, 1997 and references therein) and the common problem to relate the zircon and monazite ages to structures and metamorphic mineral assemblages, BORIANI and VILLA (1997) disqualified all geochronologic work yielding pre-Variscan ages. They argue that these ages are irrelevant to the determination of the age of D2 deformation and metamorphism or flawed by analytical problems. But, their arguments are largely selective and partially misquoted:

(1) Ordovician ages for monazite from Casletto (KÖPPEL and GRÜNENFELDER, 1971) are interpreted by BORIANI and VILLA (1997, p. 386, left middle) to date the contact metamorphism around Ordovician intrusions rather than regional metamorphism. However, there is no evidence for contact metamorphism around these intrusions (see ZINGG, 1983; HANDY, 1986; ZURBRIGGEN et al., 1997).

(2) BORIANI and VILLA (1997, p. 386, right bottom) argue that U–Xe ages (RAGETTLI, 1993) are hampered by uncertainties for the true value of the fission constant and the small analytical reproducibility (scatter among different zircon and monazite fractions from the same sample), and that therefore the U–Xe ages are irrelevant. However, BORIANI and VILLA (1997) do not mention that aliquots of the zircon and monazite samples used for Xe–U dating also have been dated with the U–Pb method. All these monazite and zircon samples yield Ordovician U–Pb ages (RAGETTLI, 1993), i.e., 457 ± 4 Ma (Giumello gneiss), 456 ± 4 Ma (Ceneri gneiss), and 452 ± 3 Ma (paragneiss from Ruspesso). Actually, combined U–Pb and U–Xe data were used to estimate the fission constant since it had become obvious that the value estimated from uranium oxides, which are potentially succeptible to loss of fissogenic Xe, and the one derived from chemically more stable silicate and phosphate minerals differ (cf. EIKENBERG et al., 1993; RAGETTLI, 1993; RAGETTLI et al., 1994).

(3) Monazite and zircon in dry systems have a high retentivity for lead and may therefore remain closed systems in amphibolite facies and lower grade metamorphism (e.g., MEZGER and KROGHSTAD, 1997; DAHL, 1997). In the presence of fluids, the U–Pb system of these minerals may behave as an open or partially open system, as these minerals can recrystallize (e.g., LEE, 1993;

TEUFEL and HEINRICH, 1997). BORIANI and VILLA (1997) argue that zircon and monazite ages for some samples, because of the high blocking temperature of these minerals, are derived from inherited components. Other zircon ages originally interpreted to reflect Ordovician high-grade metamorphism (KÖPPEL and GRÜNENFELDER, 1971) are reinterpreted by BORIANI and VILLA (1997) to date diagenesis, whereas the high-grade metamorphism would have gone by unrecorded by the U–Pb system of these zircon samples (BORIANI and VILLA, 1997, p. 386, right top).

The new staurolite data helps to resolve this controversy as staurolite represents (1) a major constituent of S2 structures (as used by ZURBRIGGEN et al., 1997), (2) has a blocking temperature for the U–Pb system that is higher than the thermal maximum experienced by its host rock (see DAHL, 1997), and (3) has no inherited components. The Pb systematics proves an Ordovician age for the growth of staurolite and a Variscan age for partial lead loss along presumably structurally controlled sites. The Variscan lead loss from staurolite implies that the $^{206}Pb/^{238}U$ ages at 385 ± 6 Ma and 360 ± 3 Ma are minimum ages for staurolite crystallization and minimum ages for the metamorphic event related with S2 structures in the SCZ. The best age estimate for this pre-Variscan metamorphism is given by published U–Pb zircon and monazite ages (457 ± 4 Ma, 456 ± 4 Ma, RAGETTLI [1993] and 450 ± 10, KÖPPEL and GRÜNENFELDER [1971]). The Permo-Carboniferous minimum age given from the readily leached staurolite-lead demonstrates a second metamorphic event, which agrees with the large number of K–Ar, ^{39}Ar–^{40}Ar, and Rb–Sr mica and amphibole ages (for a compilation see HUNZIKER et al., 1992). Therefore, the metamorphic and structural memory of the SCZ was acquired during at least two unrelated orogenic events and refutes models that rule out a pre-Variscian structural and metamorphic history of the SCZ.

Conclusions

Staurolite is an essential phase of the mineral assemblage that formed during the metamorphism related with deformation D2, which is the major metamorphic event in the sampled part of the SCZ. The U–Pb systematics of staurolite clearly demonstrates that this tectonometamorphic event occurred during the Ordovician. Therefore, the Variscian ^{39}Ar–^{40}Ar ages on mica and amphibole are associated with the S3 (S2 in BORIANI and VILLA, 1997) event, having crystallized or having been thermally overprinted and reset during this event. Furthermore, BORIANI and VILLA's (1997) assertions of zircon recrystallization during Ordovician "diagenesis" (p. 386), apparently an opinion held by a minority of one, is not compatible with the staurolite age data. Similarly, their reinterpretation and affirmation that the ages obtained by the U–Xe method indicate a Variscian event rather than an Ordovician event, lacks support. Instead, the staurolite age data confirm and support earlier work demonstrating Ordovician metamorphism in the SCZ (e.g., PIDGEON et al., 1970; KÖPPEL and GRÜNENFELDER, 1971, 1978; KÖPPEL, 1974; RAGETTLI, 1993).

Acknowledgement

We thank M. Boche and J. Müller for separation of the staurolite. We gratefully acknowledge discussion and comments by M. Handy (Giessen) and constructive and detailed reviews by V. Köppel and U. Schaltegger (both Zürich).

References

BERTOLANI, M. (1959): La formazione basica "Ivrea-Verbano" e la sua posizione nel quadro geologico-petrografico della Basse Valsesia del Biellese. Per. Mineral., 28, 151–209.

BOHLEN, S.R. and LIOTTA, J.J. (1986): A barometer for garnet amphibolites and garnet granulites. J. Petrol., 27, 1025–1034.

BORIANI, A. and PEYRONEL PAGLIANI, G. (1968): Rapporti fra le plutoniti erciniche e le metamorfiti del "Massiccio dei Laghi" nella zona del M. Cerano (bassa Val d'Ossola). Rend. Soc. Ital. Mineral. Petrol., 24, 111–142.

BORIANI, A. and SACCHI, R. (1973): Geology of the junction between the Ivrea-Verbano and Strona-Ceneri Zone. Mem. Ist. Geol. Univ. Padova, 28, 1–36.

BORIANI, A. and VILLA, I.M. (1997): Geochronology and regional metamorphism in the Ivrea-Verbano Zone and Serie dei Laghi, Italian Alps. Schweiz. Mineral. Petrogr. Mitt., 77, 381–401.

BORIANI, A., ORIGONI GIOBBI, E., BORGHI, A. and CAIRONI, V. (1990): The evolution of the "Serie dei Laghi" (Strona-Ceneri and Schisti dei Laghi): the upper component of the Ivrea-Verbano crustal section; Southern Alps, North Italy and Ticino, Switzerland. Tectonophysics, 182, 103–118.

CAPEDRI, S. (1971): Sulle rocce della formazione basica Ivrea-Verbano. 2. Petrografia della granuliti e rocce derivate affioranti nella Val Mastallone (Vercelli) e loro evoluzione petrogenetica. Mem. Soc. Geol. Ital., 10, 277–312.

DAHL, P.S. (1997): The crystal-chemical basis for differential retention of Pb among geochronometric silicates and phosphates. Earth Planet. Sci. Lett., 150, 277–290.

EIKENBERG, J., SIGNER, P. and WIELER, R. (1993): U–Xe, U–Kr, and U–Pb systematics for dating uranium minerals and investigations of the production of nucleogenic neon and argon. Geochim. Cosmochim. Acta, 57, 1053–1069.

FRANZ, L., TEUFEL, S. and ONCKEN, O. (1994): Die Abkühlungsgeschichte orogen gestörter Kruste –

das Ivrea-Krustensegment (Norditalien), erste Ergebnisse, Göttinger Arbeiten zur Geologie und Paläontologie, 1, 129–131.

FRANZ, L., HENK, A., TEUFEL, S. and ONCKEN, O. (1996): Metamorphism in the Ivrea and Strona-Ceneri Zones (Northern Italy): Thermobarometry, geochronology and inferences about the crustal evolution. – In: Structure and properties of high strain zones in rocks. Verbania. Abstr. Vol., 69.

FREY, R., BIINO, G.G. and PROSPERT, C. (1995): Dating a Variscan pressure-temperature loop with staurolite. Geol., 23, 1095–1098.

FREY, R. and KAMBER, B.S. (1995): Single mineral Pb–Pb dating. Earth Planet. Sci. Lett., 129, 261–268.

FREY, R., VILLA, I.M., KRAMERS, J.D., NÄGLER, T.F., PRZYBYLOWICZ, W.J., PROZESKY, V.M., HOFMANN, B. and KAMBER, B.S. (1997): Single mineral dating by the Pb–Pb step-leaching method: assessing the mechanisms. Geochim. Cosmochim. Acta, 61, 393–414.

GHENT, E.D., STOUT, M.Z., BLACK, P.M. and BROTHERS, R.N. (1987): Chloritoid bearing rocks with blueschists and eclogites, northern New Caledonia. J. Metam. Petrol., 5, 239–254.

GERSTENBERGER, H. and HAASE, G. (1997): A highly effective emitter substance for mass spectrometric Pb isotope ratio determinations. Chem. Geol., 136, 309–312.

HANDY, M.R. (1986): The structure and rheological evolution of the Pogallo fault zone, a deep crustal dislocation in the Southern Alps of northwestern Italy (prov. Novara). Unpubl. Ph. D. Thesis, University of Basel, Switzerland.

HANDY, M.R. (1987): The structure, age and kinematics of the Pogallo fault line, southern Alps, northwestern Italy. Eclogae geol. Helv., 80, 593–632.

HANDY, M.R. and ZINGG, A. (1991): The tectonic and rheological evolution of an attenuated cross section of the continental crust: Ivrea crustal section, southern Alps, northwestern Italy and southern Switzerland. Geol. Soc. Am., Bull. 103, 236–253.

HANDY, M.R., FRANZ, L., HELLER, F., JANOTT, B. and ZURBRIGGEN, R. (in press): Multistage accretion, orogenic stacking, and exhumation of continental crust (Ivrea crustal section, Italy and Switzerland). Tectonics.

HENK, A., FRANZ, L., TEUFEL, S. and ONCKEN, O. (1997): Magmatic underplating, extension and crustal reequilibration – insights from a cross section through the Ivrea Zone and Strona-Ceneri Zone / northern Italy. J. Geol. 105, 367–377.

HODGES, K.V. and FOUNTAIN, D.M. (1984): Pogallo Line, South Alps, Northern Italy: an intermediate crustal level, low-angle normal fault. Geology, 12, 151–155.

HODGES, K.V. and SPEAR, F.S. (1982): Geothermometry, geobarometry and the Al_2SiO_5 triple point at Mt. Moosilauke, New Hampshire. Am. Mineral., 67, 1118–1134.

HOISCH, T.D. (1989): Empirical calibration of six geobarometers for the assemblage quartz + muscovite + biotite + plagioclase + garnet. Contrib. Mineral. Petrol., 104, 225–234.

HUNZIKER, J.C., DESMONS, J. and HURFORD, A.J. (1992): Thirty-two years of geochronological work in the Central and Western Alps: a review on seven maps. Mémoires de Géologie (Lausanne), 13, 59 pp.

JAFFEY, A.H., FLYNN, K.F., GLENDENIN, L.F., WENTLY, W.C. and ESSLING, A.M. (1971): Precision measurements of halv-lives and specific activities of ^{235}U and ^{238}U. Phys. Rev., C4, 1889–1906.

KÖPPEL, V. (1974): Isotopic U–Pb ages of monazites and zircons from the crust-mantle transition and adjacent units of the Ivrea and Ceneri Zones (Southern Alps, Italy). Contrib. Mineral. Petrol., 43, 55–70.

KÖPPEL, V. and GRÜNENFELDER, M. (1971): A study of inherited and newly formed zircons from paragneisses and granitized sediments of the Strona-Ceneri Zone (Southern Alps). Schweiz. Mineral. Petrogr. Mitt., 51, 385–410.

KÖPPEL, V. and GRÜNENFELDER, M. (1978): Monazite and zircon U–Pb ages from the Ivrea and Ceneri zones. Mem. Ist. Sci. Geol. Univ. Padova, 33, 257 (abstr.).

KULLERUD, L. (1991): On the calculation of isochrons. Chem. Geol., 87, 307–316.

LEE, J.K.W. (1993): Problems and progress in the elucidation of U and Pb transport mechanisms in zircon. In: BOLAND, J.N. and FITZGERALD, J.D. (eds): Defects and processes in the solid state: geoscience applications, the McLaren volume. Elsevier, Amsterdam, 423–446.

LUDWIG, K.R. (1994): ISOPLOT – A plotting and regression program for radiogenic-isotope data. Version 2.71. U.S. Geol. Surv. Open-File Report 91-445 (revised 1994).

MANHÈS, G., MINSTER, J.F. and ALLÈGRE, C.J. (1978): Comparative uranium-thorium-lead and rubidium-strontium study of the Saint Séverin amphoterite: consequences for early solar chronology. Earth Planet. Sci. Lett., 39, 14–24.

MCDOWELL, F.W. (1970): Potassium-Argon ages from then Ceneri Zone, southern Swiss Alps. Contrib. Mineral. Petrol., 28, 165–182.

MEZGER, K. and KROGHSTAD, E.J. (1997): Interpretation of discordant U–Pb zircon ages: An evaluation. J. Metam. Geol., 15, 127–140.

PERCHUK, L.L. (1969): The staurolite-garnet-geothermometer. Dokladie Akad SSSR, 186, 1405–1407; in Russian.

PIDGEON, R.T., KÖPPEL, V. and GRÜNENFELDER, M. (1970): U–Pb isotopic relationships in zircon suites from a para- and ortho-gneiss from the Ceneri zone, southern Switzerland. Contrib. Mineral. Petrol., 26, 1–11.

PINARELLI, L., BORIANI, A. and DEL MORO, A. (1988): Rb–Sr geochronology of the Lower Permian plutonism in Massiccio dei Laghi, Southern Alps (NW Italy). Rend. Soc. Ital. Mineral. Petrol., 43, 411–428.

POWELL, R. and HOLLAND, T.J.B. (1988): An internally consistent dataset with uncertainties and correlations: 3. Applications to geobarometry, worked examples and a computer program. J. Metam. Geol., 6, 173–204.

POWNCEBY, M.I., WALL, V.J. and O'NEILL, H.ST.C. (1987a): Fe–Mn partitioning between garnet and ilmenite: experimental calibration and applications. Contrib. Mineral. Petrol., 97, 116–126.

POWNCEBY, M.I., WALL, V.J. and O'NEILL, H.ST.C. (1987b): Fe–Mn partitioning between garnet and ilmenite: experimental calibration and applications (correction). Contrib. Mineral. Petrol., 97, 539.

RAGETTLI, R.A. (1993): Vergleichende U–Xe- und U–Pb-Datierung an Zirkon und Monazit. Ph. D. Diss. ETH Zürich No. 10183, 139 pp.

RAGETTLI, R.A., HEBEDA, E.H., SIGNER, P. and WIELER, R. (1994): Uranium-Xenon chronology: precise determination of λ_{sf^*}, $^{136}Y_{sf}$ for spontaneous fission of ^{238}U. Earth Planet. Sci. Lett., 128, 653–670.

ROMER, R.L. and BRIDGWATER, D. (1997): Geochronologic significance of lead lines from old cratons. Chem. Geol., 136, 125–133.

SCHIØTTE, L. (1989): On the possible role of fluid trans-

port in the distribution of U and Pb in an Archaean gneiss complex. In: BRIDGWATER, D. (ed.): Fluid Movements – Element Transport and Composition of the Deep Crust. NATO (N. Atlantic Treaty Org.), Adv. Sci. Inst., Ser. C: Math. Phys. Sci., 281: 299–317.

SCHMID, S.M. (1993): Ivrea Zone and adjacent southern Alpine basement. In: VON RAUMER, J.F. and NEUBAUER, F. (eds): Pre-Mesozoic geology in the Alps, Springer, Berlin, 567–583.

SPEAR, F.S. and CHENEY, J.T. (1989): A petrogenetic grid for pelitic schists in the system SiO_2–Al_2O_3–FeO–MgO–K_2O–H_2O. Contrib. Mineral. Petrol., 101, 149–164.

STEIGER, R.H. and JÄGER, E. (1977): Subcommission on geochronology: Convention on the use of decay constants in geo- and cosmochronology. Earth Planet. Sci. Lett., 36, 359–362.

TEUFEL, S. and HEINRICH, W. (1997): Partial resetting of the U–Pb isotope system in monazite through hydrothermal experiments: An SEM and U–Pb study. Chem. Geol., 137, 273–281.

TILTON, G.R. (1973): Isotopic lead ages of chondritic meteorites. Earth Planet. Sci. Lett., 19, 321–329.

VAVRA, G., GEBAUER, D., SCHMID, R. and COMPSTON, W. (1996): Multiple zircon growth and recrystallization during polyphase Late Carboniferous to Triassic metamorphism in granulites of the Ivrea Zone (Southern Alps): an ion microprobe (SHRIMP) study. Contrib. Mineral. Petrol., 122, 337–358.

VON QUADT, A., FERRARIO, A., DIELLA, V., HANSMANN, W., VAVRA, G. and KÖPPEL, V. (1993): Zircon U–Pb ages from chromites of the phlogopite peridotite of Finero, Ivrea Zone. Terra Abstracts, 5(1), 393–394.

ZINGG, A. (1983): The Ivrea and Ceneri-Strona zones (Southern Alps, Ticino and N-Italy) – a review. Schweiz. Mineral. Petrogr. Mitt. 63, 361–392.

ZINGG, A. (1990): The Ivrea crustal cross-section (northern Italy and southern Switzerland). In: SALISBURY, M.H. and FOUNTAIN, D.M. (eds): Exposed Cross-Sections of the Continental Crust. NATO (N. Atlantic Treaty Org.), Adv. Sci. Inst., Ser. C: Math. Phys. Sci., 317, 1–20.

ZINGG, A., HANDY, M.R., HUNZIKER, J.C. and SCHMID, S.M. (1990): Tectonometamorphic history of the Ivrea Zone and its relationship to the crustal evolution of the Southern Alps. Tectonophysics, 182, 169–192.

ZURBRIGGEN, R., FRANZ, L. and HANDY, M.R. (1997): Pre-Variscan deformation, metamorphism and magmatism in the Strona-Ceneri Zone (southern Alps of northern Italy and southern Switzerland). Schweiz. Mineral. Petrogr. Mitt., 77, 361–380.

ZURBRIGGEN, R., KAMBER, B.S., HANDY, M.R. and NÄGLER, T.F. (1998): Dating syn-magmatic folds: A case study of Schlingen structures in the Strona-Ceneri Zone (Southern Alps, northern Italy). J. Metam. Geol.

Manuscript received February 15, 1998; revision accepted June 22, 1998.